analytical chemistry

Article

pubs.acs.org/ac

Design and Biosensing of Mg^{2+}-Dependent DNAzyme-Triggered Ratiometric Electrochemiluminescence

Yan Cheng, Yin Huang, Jianping Lei,* Lei Zhang, and Huangxian Ju

State Key Laboratory of Analytical Chemistry for Life Science, School of Chemistry and Chemical Engineering, Nanjing University, Nanjing 210093, People's Republic of China

ABSTRACT: A dual-potential ratiometric electrochemiluminescence (ECL) sensing approach based on Mg^{2+}-dependent DNAzyme-regulated ECL signals of luminol and CdS quantum dots (QDs) is designed. The system consists of DNAzyme strand functionalized QDs as capture probes and cathode ECL emitters, luminol-reduced gold nanoparticles (Au@luminol) as anode ECL emitters, and a Mg^{2+} substrate strand modified with a cyanine dye (Cy5) fluorophore as the quencher. In the absence of Mg^{2+} ions, the cathode ECL of the QDs is quenched by electrochemiluminescence resonance energy transfer between CdS QDs and Cy5 molecule, while the anode ECL from Au@luminol is introduced into the system. On the other hand, in the presence of Mg^{2+} ions, the DNAzyme cleaves the substrate strand, and then releases the Cy5 and Au@luminol, which results in the recovery of the cathode ECL of the QDs and the decrease of the anode ECL simultaneously. On the basis of the ratio of ECL intensities at two excitation potentials, this approach was demonstrated to yield a linear calibration range from 10 to 10 000 μM Mg^{2+} before it was applied to Mg^{2+} detection in Hela cell extract. DNAzyme-triggered ratiometric ECL strategy with potential resolution would provide a reliable and sensitive method in biosensing and clinical diagnosis.

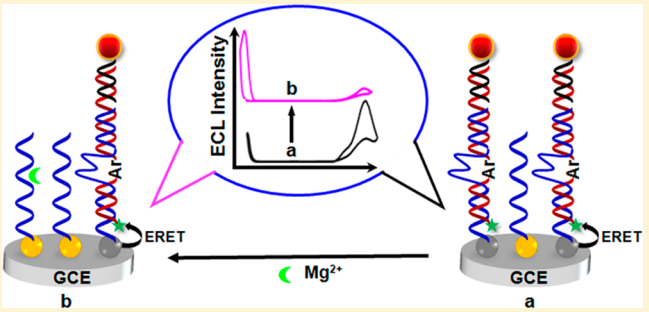

Electrochemiluminescence (ECL) is an electrochemically triggered optical radiation process produced by the energy relaxation of excited species.[1−3] Due to the separation between the applied voltage and the ECL emission, this technique is a promising tool that has attracted much attention in sensing and detecting trace amounts of samples.[4−7] The conventional ECL methods have been established on the basis of steric hindrance from biorecognition reaction,[8,9] generation/consumption of coreactant in enzyme catalytic reactions,[10,11] and ECL resonance energy transfer.[12,13] However, since the detection signal is only a change in ECL intensity, other factors such as environmental conditions can interfere with the signal output. Thus, there is a persistent research motivation to seek for an efficient ECL system/platform combined with novel mechanism and/or modern analytical technique.[14−17] Considering most ECL nanoemitters are capable of photoluminescence (PL) emission, it is natural to adapt their PL strategies concerning about the ratiometric fluorescence into ECL systems, giving rise to the methodology of ratiometric ECL, which can eliminate most ambiguities by self-calibration of two emission bands.[18] An ECL ratiometric sensing approach has been developed via consumption of coreactant for DNA detection,[19] but the requirement of luminol-modified target DNA as an anode ECL emitter is limited in practical applications.

Recently, ECL technology has made significant progresses in many fields by integrating with nanomaterial-based signal transduction,[20,21] biologically molecular recognition,[22,23] and enzymatic catalysis.[24,25] In particular, DNAzymes as enzyme mimics have attracted considerable attention in ECL techniques due to their high catalytic activity and good stability.[26,27] On the basis of the consumption of dissolved O_2 by the assembled hemin/G-quadruplex DNAzymes, a highly sensitive ECL strategy was designed for the detection of ochratoxin A in an oxygen/persulfate system.[28] On the other hand, the base sequences of DNAzymes can specifically bind with metal ions to form metal-dependent DNAzyme and exhibit catalytic capacity for cleaving ribonucleic acid targets.[29−32] Combining the high selectivity of DNAzyme with the high sensitivity of ECL, a DNAzyme-based ECL sensor has been reported for the detection of Pb^{2+} with a low detection limit of 11 pM.[33] Further, a functionalized paper-based ECL device was developed for simultaneous detection of Pb^{2+} and Hg^{2+} through the formation of G-quadruplex and T−Hg−T complex, respectively.[34] Here, based on the specific recognition toward target analytes and catalytic reaction of DNAzyme, a DNAzyme-triggered ratiometric ECL strategy is designed for the first time to detect magnesium ion (Mg^{2+}) in complex samples.

Mg^{2+} is an alkaline earth metal that plays diverse roles in the human body as well as biological activities.[35] However, due to its light metal property and lack of specific recognizing probe,

Received: March 17, 2014
Accepted: April 28, 2014
Published: April 28, 2014

   dx.doi.org/10.1021/ac500965p | *Anal. Chem.* 2014, 86, 5158−5163

there are limited efficient detection methods for Mg^{2+}. In this work, a novel ratiometric ECL sensing approach is developed by Mg^{2+}-dependent DNAzyme-regulated ECL emission of luminol loaded on gold nanoparticles (Au@luminol) and CdS quantum dots (QDs) as two different ECL emitters (Scheme 1). First, a Mg^{2+} substrate strand (DNA2) modified with a

Scheme 1. Schematic Representation of Ratiometric Electrochemiluminescence Strategy Triggered by Mg^{2+}-Dependent DNAzyme for Biosensing

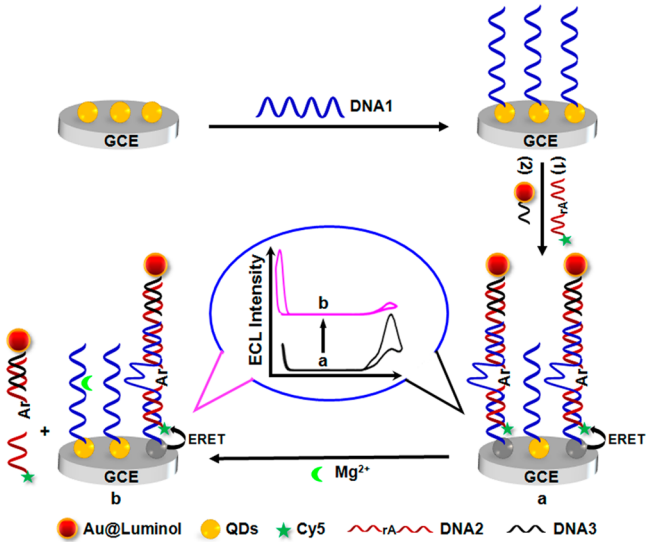

cyanine dye (Cy5) fluorophore as the acceptor is designed. After hybridization with capture probe (DNA1) and sequentially with signal DNA (DNA3), the Au@luminol is introduced in the ECL system, which results in the enhanced anode ECL. Meanwhile, the cathode ECL of the QDs at a different excitation potential is quenched by electrochemiluminescence resonance energy transfer (ERET) between CdS QDs and Cy5 molecule. After adding Mg^{2+} in the system, Mg^{2+}-dependent DNAzyme could be formed, and this will cleave the substrate strand, which generates small oligonucleotide fragments to release the Cy5 and Au@luminol. Thus, the cathodic ECL of the QDs is recovered, and the anodic ECL decreases simultaneously. On the basis of the ratio of two ECL intensities, this approach exhibits good performance in the detection of Mg^{2+} and has been applied to the detection of Mg^{2+} in Hela cell extract. The DNAzyme-based ratiometric ECL strategy provides a precise and reliable analytical method in complex samples and expands the ECL application in bioanalysis.

EXPERIMENTAL SECTION

Materials and Reagents. Bovine serum albumin (BSA), mercaptopropionic acid (MPA), luminol, thioacetamide, tris(2-carboxyethyl)phosphine hydrochloride solution (TCEP, 0.5 M), 1-ethyl-3-(3-(dimethylamino)propyl) carbodiimide (EDC), and tris(hydroxymethyl)aminomethane (Tris) were obtained from Sigma-Aldrich Chemical Co. (St. Louis, MO). Magnesium chloride ($MgCl_2·6H_2O$) was purchased from Xilong Chemical Co., Ltd. Cadmium chloride ($CdCl_2·2.5H_2O$) was purchased from Alfa Aesar China Ltd. 6-Mercapto-1-hexanol (MCH) was purchased from Nanjing Chemical Reagent Co., Ltd. Chloroauric acid ($HAuCl_4·4H_2O$) was obtained from Shanghai Reagent Co. (Shanghai, China). Cell lysis buffer was purchased from Millipore, U.S.A. In our work, 0.1 M phosphate buffer salines (PBS) at various pHs were prepared by mixing the stock solutions of 0.1 M NaH_2PO_4 and 0.1 M Na_2HPO_4 containing 0.1 M KNO_3 as the supporting electrolyte. Ultrapure water obtained from a Millipore water purification system (≥18 MΩ, Milli-Q, Millipore) was used throughout the work.

The DNA constructs were synthesized by Shanghai Sangon Biotechnology Co. Ltd. (Shanghai, China). All oligonucleotides were purified using high-performance liquid chromatography and were diluted to give stock solutions of 5 μM in 0.1 M Tris–HCl (pH 7.4). The sequences of three oligomers are given as follows: DNA1 as DNAzyme strand, 3′-*AAG AGA* GTG TAC CCA CGG CAA GGC CTA GCG A*CT GTT TT*–$(CH_2)_6$–NH_2-5′; DNA2 as substrate strand, 5′-**CTT CTT CTT CTA TG***T TCT CTC* TrAG *GAC AAA A*–$CH_2)_6$–Cy5-3′ ("rA" denotes an A base of RNA); DNA3 as signal strand, 3′-HS–$(CH_2)_6$–**GAA GAA GAA GAT AC**-5′.

Apparatus. The transmission electron micrographs (TEMs) were obtained using a JEM-2100 TEM instrument (JEOL, Japan). Dynamic light scattering (DLS) measurements were performed by BI-200SM light scattering apparatus (Brookhaven Instruments Co., U.S.A.) equipped with a digital correlator at 640 nm. UV–vis absorption spectra were obtained with a UV-3600 UV–vis–NIR spectrophotometer (Shimadzu Co., Kyoto, Japan). Electrochemiluminescent measurements were carried out on a MPI-E multifunctional electrochemical and chemiluminescent analytical system (Xi'an, China), with a modified glassy carbon electrode (GCE, 5 mm in diameter, China) as a working electrode, a platinum wire as a counter electrode, and a Ag/AgCl (saturated KCl) as a reference electrode. The ECL emission window was placed in front of the photomultiplier tube (PMT, detection range from 300 to 650 nm) biased at 1000 V with scan rate of 100 mV s^{-1}.

Preparation of MPA-Capped CdS QDs. The water-soluble CdS QDs were prepared using MPA as a stabilizing agent according to a previously reported method.[36] Briefly, 86 μL of MPA was added to 20 mL of 20 mM $CdCl_2$ solution. The pH of the solution was adjusted to 10 using 1 M sodium hydroxide. Then, 20 mL of 20 mM aqueous thioacetamide solution was added with extensive stirring in air for 30 min. After being refluxed at 80 °C for 10 h, the formed CdS colloid was dialyzed exhaustively against water overnight at room temperature to obtain CdS QDs solution. Finally, the product was kept at 4 °C.

Synthesis of Au@luminol. The Au@luminol nanohybrids with an average diameter of 20 nm were synthesized by a one-pot method according to reference with some modification.[37] All glassware used in the following procedures was cleaned in a bath of freshly prepared HNO_3/HCl (3:1, v/v), rinsed thoroughly in redistilled water, and dried prior to use. Gold colloids were prepared by the reduction of $HAuCl_4$ with luminol. A 100 mL portion of $HAuCl_4$ solution (0.01%, w/w) was heated to boiling point. With stirring vigorously, 1.6 mL of 0.01 M luminol was added rapidly. When the solution was maintained at boiling point for 30 min, a color change from yellow to wine-red was observed. The heating source was removed, and the colloid was kept at room temperature for another 20 min and then stored at 4 °C.

Preparation of Au@luminol–DNA3 Conjugates. Initially, 250 μL of 5% BSA solution was added to 1 mL of pH 7.0 Au@luminol solution and incubated at room temperature for 0.5 h to block the Au@luminol. Then, the Au@luminol was

dx.doi.org/10.1021/ac500965p | Anal. Chem. 2014, 86, 5158–5163

centrifuged at 12 000 relative centrifugal force (rcf) for 10 min and the red precipitates were dispersed with 300 μL of Tris−HCl buffer. Meanwhile, 35 μL of 100 nM thiolated DNA3 and 15 μL of 10 mM TCEP were mixed and incubated at room temperature for 0.5 h. Then the mixture was added to the Au@luminol solution and incubated at room temperature for 4 h. The as-prepared mixture was centrifuged at 10 000 rcf for 5 min, and the red precipitates were suspended with 300 μL of Tris−HCl buffer. Sequentially, 30 μL of 10 mM MCH solution was added and incubated at 37 °C for 0.5 h to block the Au@luminol−DNA3 conjugates and optimize the orientation of DNA3 to form a mixed monolayer, making the hybridization easier and preventing the nonspecific adsorption of Au nanoparticles (AuNPs) surface.

Fabrication of Ratiometric ECL Biosensor. First the GCE was polished successively with 1.0 and 0.05 μm alumina slurry (Beuhler). After successive sonication in acetone and deionized water, the electrode was dried under N_2. Before modification, QDs solution was condensed by ultrafiltration at 10 000 rcf for 10 min, and the upper phase was decanted and then dissolved in 20 μL of water and applied to the GCE. The formed QD film was stable due to the low solubility and strong physical adsorption of QDs on the surface of GCE. Finally, the CdS QDs-modified GCE was stored in 0.1 M Tris−HCl buffer (pH 7.4) containing 0.1 M NaCl for characterization and further use.

ECL Detection. To activate carboxylic acid groups of CdS QDs, the CdS QDs-modified electrode was immersed in 1 mL of Tris−HCl buffer (pH 7.4) containing 20 mM EDC for 1 h at room temperature and then washed with 0.1 M pH 7.4 Tris−HCl solution. Next, 20 μL of DNA1 was spread on the preprepared electrode surface at 37 °C for 1 h and 4 °C overnight in a 100% moisture-saturated environment. The resulting electrode surface was slowly washed with a stream of 0.01 M pH 7.4 Tris−HCl solution to remove unbound oligonucleotides. Then the Cy5-DNA2 and Au@luminol−DNA3 were sequentially hybridized on the electrode surface at 37 °C for 30 and 40 min, respectively. To cleave Mg^{2+}-dependent DNAzyme, the resulting electrode was incubated in 10 mM $MgCl_2$ solution for 50 min. Finally, the as-prepared biosensor was rinsed three times with deionized water before it was used in ECL measurements in air-saturated PBS with 6.5 mM H_2O_2 as coreactant.

Cell Extract. Cells were collected in the exponential phase of growth, and 5×10^7 cells were dispensed in a 1.5 mL Eppendorf tube, washed twice with ice-cold PBS (0.1 M, pH 7.4), and resuspended in 500 μL of ice-cold 3-[(3-cholamidopropyl)dimethylammonio]-1-propanesulfonate (CHAPS) lysis buffer containing 20 mM Tris−HCl (pH 7.2), 0.1 M NaCl, 1 mM EDTA, 10 mM dithiothreitol, 0.5% CHAPS, and 10% sucrose. The mixture was incubated for 30 min in ice and centrifuged at 14 000 rcf at 4 °C for 20 min. The supernatant was collected as cell extract for analysis or frozen at −80 °C.

RESULTS AND DISCUSSION

Characterization of Au@luminol and CdS QDs. The topographies and sizes of the obtained Au@luminol and CdS QDs were characterized with high-resolution TEM images. The typical TEM images of Au@luminol (Figure 1A) and CdS QDs (Figure 1B) showed a homogeneous distribution of around 20 and 6 nm in diameter, respectively. The good dispersibility and stability of the Au@luminol have been evaluated from DLS analysis. This size of Au@luminol approximated the mean hydrodynamic diameter of 22 nm (Figure 1C). After the Au@luminol−DNA3 composite was fabricated via Au−S chemistry, the resulting hydrodynamic diameter is 29 nm (Figure 1D). These results suggested no massive aggregation of Au@luminol and Au@luminol−DNA3 composite in aqueous solution. The increase of hydrodynamic diameter of the Au@luminol−DNA3 composite indicated that DNA was conjugated to the Au@luminol surface.

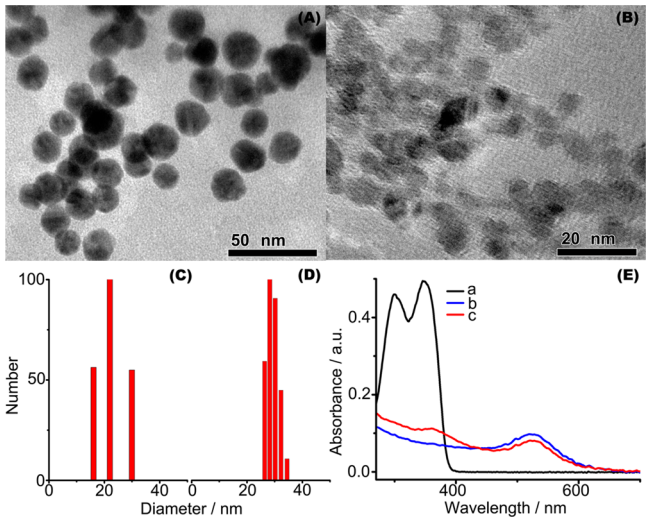

Figure 1. HRTEM images of (A) Au@luminol and (B) CdS QDs. The hydrodynamic sizes of (C) Au@luminol and (D) Au@luminol−DNA3 composite measured by DLS. (E) UV−vis spectra of luminol (a), 13 nm AuNPs (b), and Au@luminol (c).

UV−vis spectra were used to characterize the formation of Au@luminol (Figure 1E). The spectrum of luminol solution exhibited its characteristic peaks at around 300 and 360 nm (curve a) and the spectrum of 13 nm AuNPs synthesized with sodium citrate as a stabilizer showed an absorption peak at 525 nm (curve b). When the AuNPs synthesized in luminol solutions, it can be seen that the dual absorption peaks of luminol have almost disappeared in the UV−vis spectrum of the Au@luminol colloid and two absorption peaks at 365 and 530 nm appeared (curve c), which is consistent with the data described previously,[37] indicating that luminol functionalized AuNPs have been prepared. The high-density luminol on AuNPs is beneficial to enhance the anode ECL emission.

Feasibility of Ratiometric ECL Biosensor. In order to confirm the feasibility of the method, ECL−potential responses were investigated stepwise, and the results are shown in Figure 2A. The QDs-modified electrode showed an intensive cathode ECL emission peak at −1.26 V in air-saturated pH 8.0 PBS buffer with H_2O_2 as coreactant (curve a). After immobilizing with the DNA1, the cathode ECL intensity slightly decreased by 9.3% (curve b) as a result of the increased impedance and inhibition of H_2O_2 diffusion to the electrode surface. However, after hybridizing with Cy5-DNA2 and Au@luminol−DNA3 consecutively, the QD/DNA1-modified electrode exhibited a significant 73.6% decrease in the cathode ECL intensity, and a new anode ECL peak appeared at +0.75 V (curve c). Sequentially, after adding 10 mM Mg^{2+}, the cathode ECL signal recovered to 70.5% of QD/DNA1-modified electrode but anode ECL signal decreased to 22.5% of QD/DNA1/Cy5-DNA2/Au@luminol−DNA3-modified electrode (curve d), which is attributed to the inhibition of ERET between QDs

dx.doi.org/10.1021/ac500965p | Anal. Chem. 2014, 86, 5158−5163

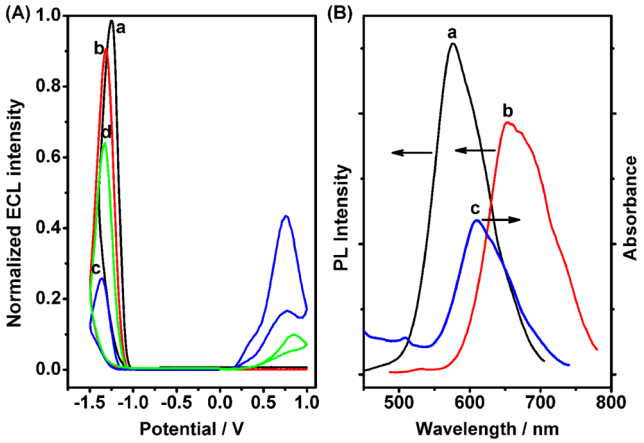

Figure 2. (A) ECL–potential curves of QDs (a), QDs/DNA1 (b), and QDs/DNA1/Cy5-DNA2/Au@luminol–DNA3 in the absence (c) and presence (d) of 10 mM Mg^{2+} in pH 8.0 PBS buffer containing 6.5 mM H_2O_2. (B) Fluorescence emission spectra of QDs (a) and Cy5 (b) and absorption spectrum of Cy5 in aqueous solution (c).

and Cy5, and the release of Au@luminol–DNA3, respectively. Therefore, the ratio of ECL intensities at two excitation potentials would be dependent on the concentrations of Mg^{2+}, which provides a possibility to design a highly sensitive and selective method for the detection of Mg^{2+}. Moreover, the dual-potential ratiometric ECL strategy could decrease the background interference in complex samples by self-calibration of two emission bands.

To further study the quenching mechanism between QDs and Cy5, the UV–vis spectrum and fluorescence emission spectra of aqueous Cy5 and QDs were obtained (Figure 2B). The fluorescence emission of QDs (curve a) significantly overlaps with the absorption spectrum of Cy5 (curve c), indicating the potential of resonance energy transfer between the excited QDs and Cy5. Moreover, the ECL emission of MPA-CdS QDs is band gap mode that the wavelength of the ECL emission is the same as that of the PL emission from the core.[38] Therefore, the ECL resonance energy transfer could be taking place between the QDs and Cy5.

Optimization of Detection Conditions. Different from the fluorescence resonance energy transfer (FRET)-based fluorescence methods, the ratiometric ECL technique generated two ECL emissions of QDs and luminol. In the absence of target Mg^{2+}, the two strands between DNA1 and DNA2 could hybridize to form a duplex structure, which led to the Cy5 close to QDs and quenching the ECL of QDs. Meanwhile, the formation of duplex structure between DNA2 and DNA3 introduced the Au@luminol on the surface of the biosensor, producing a low ECL ratio of QDs to Au@luminol (Figure 3A), in which the maximal cathode ECL intensity after the reaction of Mg^{2+}-dependent DNAzyme was chosen as a normalized base. Upon addition of target, the Mg^{2+}-dependent DNAzyme was formed, and this cleaved the substrate strand to release the Cy5 and Au@luminol, which results in a high ECL ratio of QDs to Au@luminol (Figure 3B). These results further identified the feasibility of the designed ratiometric ECL strategy. Moreover, the change rate of ECL ratio increased with the increasing of pH up to 8.0 during the ECL measurements, and then deceased at pH 9.0. Therefore, 0.1 M pH 8.0 PBS buffer was used throughout the following experiments.

To efficiently apply the ratiometric ECL system to Mg^{2+} detection, several other experimental parameters including

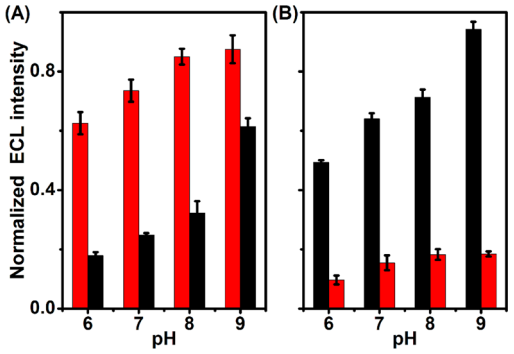

Figure 3. Effects of pH value of detection solution in the (A) absence and (B) presence of 10 mM Mg^{2+} on normalized cathode (black) and anode (red) ECL intensity at the biosensor in PBS buffer containing 6.5 mM H_2O_2.

incubation time of the hybridization and the time of Mg^{2+} reaction were optimized (Figure 4). The detection sensitivity

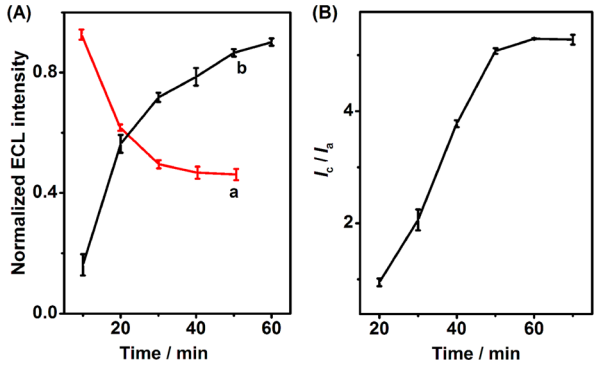

Figure 4. Effects of (A) the incubation time of the hybridization of Cy5-DNA2 with DNA1 on normalized cathode ECL intensity of QDs (a), and Au@luminol–DNA3 on normalized anode ECL intensity of luminol (b), and (B) the cleaving time of Mg^{2+}-dependent DNAzyme on the ratio of cathode to anode ECL peak intensity. When one parameter changes the others are under their optimal conditions.

depended on the formation of DNA and Mg^{2+} reaction on the electrode surface. Thus, the hybridization time of DNA and the time of the Mg^{2+} reaction are important in this method. As shown in Figure 4A, the cathode ECL signal decreased with increasing hybridization time between DNA1 and Cy5-DNA2, and then tended to a constant value after 30 min (curve a), which was attributed to the limitation of the saturated hybridization site. The hybridization time between DNA2 and Au@luminol–DNA3 was chosen to be 40 min (curve b), in which the anode ECL intensity increased slowly. In addition, the ratio of cathode to anode ECL peak intensity had no obvious change after the time of Mg^{2+} reaction reached 50 min (Figure 4B), indicating that the time was sufficient for specific reaction during the ECL detection.

ECL Responses to Mg^{2+}. The ratiometric ECL using Mg^{2+}-dependent DNAzyme as a trigger will effectively amplify the sensing signal and improve the detection sensitivity. Thus, the dual-potential ratiometric ECL method was applied to the quantitative measurement of Mg^{2+}. As shown in Figure 5, under the optimal conditions, the cathode ECL peak intensity around −1.26 V increased with the increasing of concentrations of Mg^{2+} while the anodic ECL peak intensity around +0.75 V descended (Figure 5A). As a result, a linear relationship

dx.doi.org/10.1021/ac500965p | Anal. Chem. 2014, 86, 5158–5163

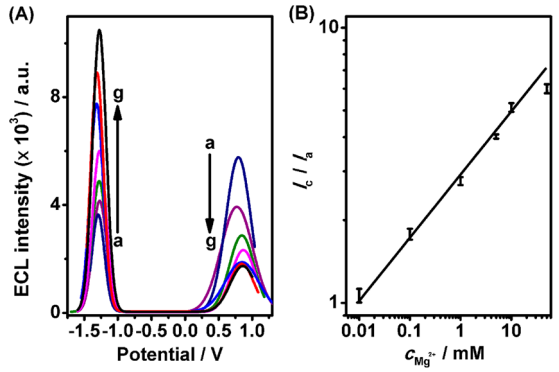

Figure 5. (A) ECL responses of the system to 0, 0.01, 0.1, 1, 5, 10, and 50 mM Mg^{2+} (from a to g) in air-saturated pH 8.0 PBS buffer. (B) Linear calibration between Mg^{2+} concentration and the ratio of cathode to anode ECL peak intensity.

between Mg^{2+} concentration and the ratio of cathode to anode ECL peak intensity (I_c/I_a) was plotted in the concentration range of 10 μM to 10 mM (Figure 5B). The regression equation was $\log(I_c/I_a) = 0.454 + 0.21 \log c$ with a correlation coefficient of 0.987;, c was the value of Mg^{2+} concentration. Meanwhile, the limit of detection (LOD) was estimated to be 2.8 μM at signal-to-noise ratio S/N = 3 without any separation and enrichment.

The detectable concentration range was much wider than those of 0.1−5 mM for a PL detection strategy based on mesoporous SiO_2 nanoparticles[32] and 0.02−0.12 mM for derivative spectrophotometry with bromopyrogallol red.[35] Meanwhile, an LOD of 2.8 μM was much lower than the 18 μM of microcolumn liquid chromatography[39] and 41.2 μM of liquid chromatography.[40] The low LOD could be attributed to the ratiometric sensing as well as the low background noise inherent in ECL detection.

Interference. To evaluate the selectivity of the present sensing system, the effects of eight cations on the ECL intensity at the biosensor were examined. As shown in Figure 6, only in

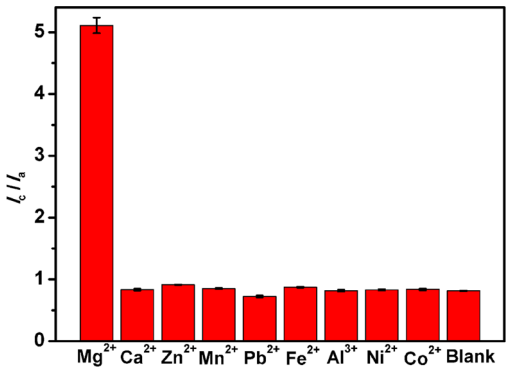

Figure 6. Ratio of cathode to anode ECL peak intensity at the biosensor in the presence of 10 mM individual metal ion in pH 8.0 PBS buffer.

the presence of Mg^{2+}, the large ratio of cathode to anode ECL peak intensity was observed, while the other cations had no obvious effect on the ratios of ECL intensity compared to the blank. These results indicate that the Mg^{2+}-dependent DNAzyme cleaves off the DNA switching units, thus enhancing the ratio of cathode to anode ECL peak intensity. Hence, the as-prepared biosensor exhibited good specificity for Mg^{2+} detection.

Reproducibility and Precision of ECL Biosensor. Ten ECL measurements of the biosensor upon continuous cyclic scans before (Figure 7A) and after (Figure 7B) the cleaving of

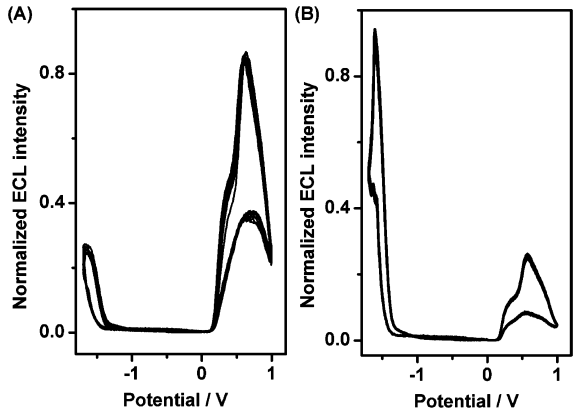

Figure 7. Continuous cyclic scans of the biosensor (A) without and (B) with the cleaving of Mg^{2+}-dependent DNAzyme in pH 8.0 PBS buffer. Scan rate: 0.1 v s^{-1}.

Mg^{2+}-dependent DNAzyme in air-saturated pH 8.0 PBS buffer showed constant signals with a relative standard deviation (RSD) of 0.99% and 1.15%, respectively, indicating the excellent stability of the modified electrode. The detection of 10 mM Mg^{2+} at three independent electrodes showed an RSD of 1.25%, giving acceptable fabrication reproducibility. When the biosensor was not in use, it was stored in air condition at 4 °C. No obvious change in the ECL intensity was observed after storage for 4 weeks, exhibiting a potential application in practice.

Detection of Mg^{2+} in Cell Extract. In order to evaluate the applicability and reliability of the present ECL system, the biosensor was used for quantifying the Mg^{2+} in Hela cells, which is a cell type in an immortal cell line. The Mg^{2+} concentration in the samples was calculated to be 0.48 ± 0.06 mM by standard addition method. When spiking with 1 and 2 mM Mg^{2+} standard solution, the average recoveries for three determinations were 93.2% ± 7.4% and 95.9% ± 10.8%, respectively, indicating good accuracy and acceptable precision.

■ CONCLUSIONS

The dual-potential ratiometric ECL strategy was designed with the use of Mg^{2+}-dependent DNAzyme as functional unit for switching the ECL signals. The two different ECL emissions were generated by QDs and Au@luminol as cathode and anode ECL emitters, respectively, resulting in the potential-resolved ECL strategy. The functional Mg^{2+} substrate strand is not only acting as an acceptor to quench the cathode ECL of QDs but also as a DNA capture to yield an anodic ECL emitter in the ratiometric ECL system. On the basis of the catalytic properties of the DNAzyme, the ratio of cathode to anode ECL peak intensity has been regulated upon the concentrations of Mg^{2+}. By integrating the specific recognition of DNAzyme toward targets with the anti-interference of ratiometric ECL, the ratiometric ECL sensing strategy was achieved with a wide linear response range, a low detection limit, and high anti-interferential capability and was successfully applied to detection of Mg^{2+} in cell extract. The DNAzyme-based

dx.doi.org/10.1021/ac500965p | Anal. Chem. 2014, 86, 5158−5163

ratiometric ECL strategy would provide a proof of concept to design a highly selective analytical approach in complex samples.

AUTHOR INFORMATION

Corresponding Author

*Phone and Fax: +86-25-83593593. E-mail: jpl@nju.edu.cn.

Notes

The authors declare no competing financial interest.

ACKNOWLEDGMENTS

This work was financially supported by the National Basic Research Program of China (2010CB732400) and National Natural Science Foundation of China (21375060, 21135002, 21121091).

REFERENCES

(1) Richter, M. M. *Chem. Rev.* **2004**, *104*, 3003−3036.
(2) Fahnrich, K. A.; Pravda, M.; Guilbault, G. G. *Talanta* **2001**, *54*, 531−559.
(3) Miao, W. J. *Chem. Rev.* **2008**, *108*, 2506−2553.
(4) Liu, S. F.; Zhang, X.; Yu, Y. M.; Zou, G. Z. *Anal. Chem.* **2014**, *86*, 2784−2788.
(5) Jie, G. F.; Wang, L.; Yuan, J. X.; Zhang, S. S. *Anal. Chem.* **2011**, *83*, 3873−3880.
(6) Li, J. P.; Li, S. H.; Wei, X. P.; Tao, H. L.; Pan, H. C. *Anal. Chem.* **2012**, *84*, 9951−9955.
(7) Li, F.; Yu, Y.; Li, Q.; Zhou, M.; Cui, H. *Anal. Chem.* **2014**, *86*, 1608−1613.
(8) Sun, B.; Qi, H. L.; Ma, F.; Gao, Q.; Zhang, C. X.; Miao, W. J. *Anal. Chem.* **2010**, *82*, 5046−5052.
(9) Pinaud, F.; Russo, L.; Pinet, S.; Gosse, I.; Ravaine, V.; Sojic, N. *J. Am. Chem. Soc.* **2013**, *135*, 5517−5520.
(10) Xu, S. J.; Liu, Y.; Wang, T. H.; Li, J. H. *Anal. Chem.* **2011**, *83*, 3817−3823.
(11) Wu, M. S.; Yuan, D. J.; Xu, J. J.; Chen, H. Y. *Anal. Chem.* **2013**, *85*, 11960−11965.
(12) Zeng, X. X.; Ma, S. S.; Bao, J. C.; Tu, W. W.; Dai, Z. H. *Anal. Chem.* **2013**, *85*, 11720−11724.
(13) Li, L.; Li, M. Y.; Sun, Y. M.; Li, J.; Sun, L.; Zou, G. Z.; Zhang, X. L.; Jin, W. R. *Chem. Commun.* **2011**, *47*, 8292−8294.
(14) Lin, X. M.; Zheng, L. Y.; Gao, G. M.; Chi, Y. W.; Chen, G. N. *Anal. Chem.* **2012**, *84*, 7700−7707.
(15) Crespo, G. A.; Mistlberger, G.; Bakker, E. *J. Am. Chem. Soc.* **2012**, *134*, 205−207.
(16) Zhang, X. W.; Chen, C. G.; Li, J.; Zhang, L. B.; Wang, E. K. *Anal. Chem.* **2013**, *85*, 5335−5339.
(17) Zhang, L.; Cheng, Y.; Lei, J. P.; Liu, Y. T.; Hao, Q.; Ju, H. X. *Anal. Chem.* **2013**, *85*, 8001−8007.
(18) Srikun, D.; Miller, S. E.; Domaille, D. W.; Chang, C. J. *J. Am. Chem. Soc.* **2008**, *130*, 4596−4597.
(19) Zhang, H. R.; Xu, J. J.; Chen, H. Y. *Anal. Chem.* **2013**, *85*, 5321−5325.
(20) Zhuo, Y.; Liao, N.; Chai, Y. Q.; Gui, G. F.; Zhao, M.; Han, J.; Xiang, Y.; Yuan, R. *Anal. Chem.* **2014**, *84*, 1053−1060.
(21) Zanarini, S.; Rampazzo, E.; Bonacchi, S.; Juris, R.; Marcaccio, M.; Montalti, M.; Paolucci, F.; Prodi, L. *J. Am. Chem. Soc.* **2009**, *131*, 14208−14209.
(22) Qi, H. L.; Li, M.; Dong, M. M.; Ruan, S. P.; Gao, Q.; Zhang, C. X. *Anal. Chem.* **2014**, *84*, 1372−1379.
(23) Zhao, P.; Zhou, L. F.; Nie, Z.; Xu, X. H.; Li, W.; Huang, Y.; He, K. Y.; Yao, S. Z. *Anal. Chem.* **2013**, *83*, 6279−6286.
(24) Deng, S. Y.; Lei, J. P.; Huang, Y.; Cheng, Y.; Ju, H. X. *Anal. Chem.* **2013**, *83*, 5390−5396.
(25) Jie, G. F.; Yuan, J. X. *Anal. Chem.* **2012**, *82*, 2811−2817.
(26) Xiao, L. J.; Chai, Y. Q.; Yuan, R.; Wang, H. J.; Bai, L. J. *Analyst* **2014**, *139*, 1030−1036.
(27) Zhou, H.; Zhang, Y. Y.; Liu, J.; Xu, J. J.; Chen, H. Y. *Chem. Commun.* **2013**, *49*, 2246−2248.
(28) Chen, Y.; Yang, M. L.; Xiang, Y.; Yuan, R.; Chai, Y. Q. *Nanoscale* **2014**, *6*, 1099−1104.
(29) Zhang, Y. F.; Yuan, Q.; Chen, T.; Zhang, X. B.; Chen, Y.; Tan, W. H. *Anal. Chem.* **2012**, *84*, 1956−1962.
(30) Wang, F.; Elbaz, J.; Teller, C.; Willner, I. *Angew. Chem., Int. Ed.* **2011**, *50*, 295−299.
(31) Wang, H. L.; Ou, L. M. L.; Suo, Y. R.; Yu, H. Z. *Anal. Chem.* **2011**, *83*, 1557−1563.
(32) Zhang, Z. X.; Balogh, D.; Wang, F.; Willner, I. *J. Am. Chem. Soc.* **2013**, *135*, 1934−1940.
(33) Zhu, X.; Lin, Z. Y.; Chen, L. F.; Qiu, B.; Chen, G. N. *Chem. Commun.* **2009**, *48*, 6050−6052.
(34) Zhang, M.; Ge, L.; Ge, S. G.; Yan, M.; Yu, J. H.; Huang, J. D.; Liu, S. *Biosens. Bioelectron.* **2013**, *41*, 544−550.
(35) Benamor, M.; Aguerssif, N. *Spectrochim. Acta, Part A* **2008**, *69*, 676−681.
(36) Han, E.; Ding, L.; Jin, S.; Ju, H. X. *Biosens. Bioelectron.* **2011**, *26*, 2500−2505.
(37) Cui, H.; Wang, W.; Duan, C. F.; Dong, Y. P.; Guo, J. Z. *Chem.—Eur. J.* **2007**, *13*, 6975−6984.
(38) Deng, S. Y.; Lei, J. P.; Yao, X. N.; Huang, Y.; Lin, D. J.; Ju, H. X. *J. Mater. Chem. C* **2013**, *1*, 299−306.
(39) Takeuchi, T.; Inoue, S.; Miwa, T. *J. Microcolumn Sep.* **2000**, *12*, 450−453.
(40) Risley, D. S.; Magnusson, L. E.; Morow, P. R.; Aburub, A. *J. Pharm. Biomed. Anal.* **2013**, *78*−*79*, 112−117.